

LNF-88/77

L. Maritato, A.M. Cucolo, R. Vaglio, C. Noce, J.L. Makous, C.M. Falco

ELECTRONIC AND SUPERCONDUCTING PROPERTIES OF Mo-Ta SUPER—
LATTICES

Estratto da: Phys. Rev. B38, 12917 (1988)

Electronic and superconducting properties of Mo-Ta superlattices

L. Maritato,* A. M. Cucolo, and R. Vaglio

Dipartimento di Fisica, Università degli Studi di Salerno, I-84100 Salerno, Italy

C. Noce

Dipartimento di Fisica Teorica e sue Metodologie per le Scienze Applicate, Università degli Studi di Salerno, I-84100 Salerno, Italy

J. L. Makous and Charles M. Falco

Department of Physics, Optical Sciences Center and Arizona Research Laboratories, University of Arizona, Tucson, Arizona 85721

(Received 15 July 1988)

We obtain bcc-bcc Mo-Ta superlattices in the modulation wavelength range 16–450 Å. The x-ray analysis shows long structural coherence even in the short-modulation-wavelength limit, and the resistivity data are in the metallic regime. We find the “universal” behavior of the T_c versus ρ curve already seen in other metals, compounds, and alloys and, for superlattices in the range 50–250 Å, the dV/dI versus V characteristics show a double-peak structure. The temperature behavior of these peaks is fitted by a two-band model and by a proximity-effect theory.

The structural, electronic, magnetic, and superconducting properties of different metallic superlattices have been intensively studied in the last few years.¹ Various combinations of elements, alloys, and compounds have been investigated, showing very interesting effects related to the layered structure, such as dimensional crossover^{2–7} or the influence of the proximity effect on the critical temperature T_c and the energy gap.^{8–12}

Ideal superlattice structures are obtained from alternating layers of two different materials, with sharp interfaces and long-range structural coherence both in the perpendicular and parallel directions relative to the plane of the substrate. The interdiffusion and the growth of interfacial alloys obviously destroy the perfect periodicity, especially in the range of short-modulation wavelengths.

Recently bcc-bcc Mo-Ta superlattices prepared by sputtering¹³ have shown structural coherence even in the monolayer limit with alternating individual atomic planes of Mo and Ta.

We have studied electronic and superconducting properties of Mo-Ta superlattices in the modulation wavelength range from 16 to 450 Å with the use of structural analysis along with critical temperature, tunneling, and resistivity measurements. We found a “universal” character of the critical temperature T_c as a function of the resistivity and we observed a double-peak structure in the dV/dI versus V characteristics of Mo-Ta based tunnel junctions in the 50–250-Å wavelength range. The temperature behavior of these two peaks was fitted both by proximity-effect theory and by two-band theory.

The layered samples were prepared with modulation such that a period consists of an equal integer number n of atomic planes of Mo and Ta, i.e., $\lambda = n [d(\text{Mo}) + d(\text{Ta})]$, where λ is the modulation wavelength and $d(\text{Mo})$, $d(\text{Ta})$ are, respectively, the interatomic distances in the actual growth direction for the Mo and Ta layers.

The Mo-Ta superlattices were deposited on sapphire

substrates using magnetically enhanced dc triode sputtering,¹⁴ with a rotating platform alternately passing over the targets. Typical pressures before sputtering were in the low 10^{-7} -Torr range and the argon pressure during the sputtering was ~ 5 mTorr. Microprocessor control of the platform rotation speed and feedback control of the sputtering rates enable constant layer thicknesses to $\pm 0.3\%$ during a deposition run.

A Bragg-Bentano geometry x-ray diffractometer with $\text{Cu } K\alpha$ radiation was used to measure directly the modulation wavelengths for samples with λ up to 150 Å. For thicker wavelengths the x-ray patterns showed two separated peaks indicating a [110] preferential growth direction for both Mo and Ta layers. In this range of values the wavelengths were calculated from the speed of the substrate table, where the calibration thicknesses were obtained using a Mirau interferometer.

In Fig. 1, as an example, the x-ray pattern of a sample with $\lambda = 87$ Å is shown. After the instrumental broadening has been deconvoluted, the structural coherence length perpendicular to the plane of the film was determined using the Scherrer equation.¹⁵ Generally this value is 4–5 times the wavelength λ of the sample. A similar method scattering off the (211) planes was used to determine the in-plane structural coherence length to be ~ 300 Å.

The resistively measured superconducting transition temperatures were sharp, with $\Delta T_c < 0.05$ K. In Fig. 2, T_c as a function of the modulation wavelength is shown. Some of the superlattices were prepared under inferior sputtering conditions and are represented by the triangles in Figs. 2 and 3.

Generally the de Gennes-Werthamer (dGW) proximity-effect theory^{16,17} well describes the decrease of T_c with λ in the region where $\lambda/2$ is larger compared to the superconducting coherence length. For the data in Fig. 2, T_c falls off faster and to a lower value than the

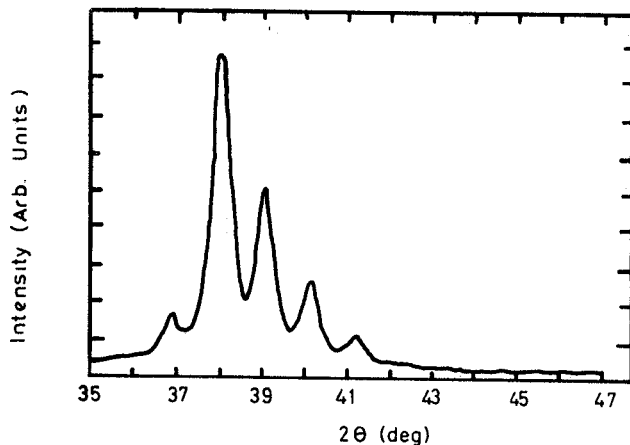


FIG. 1. Θ - 2Θ x-ray diffraction pattern of a Mo-Ta superlattice with $\lambda=87 \text{ \AA}$.

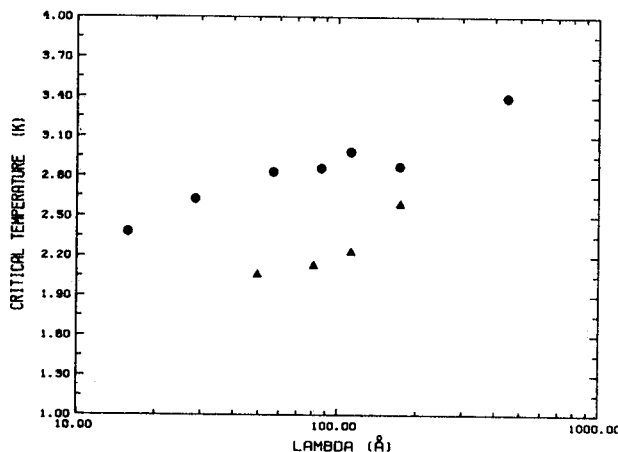


FIG. 2. Critical temperature T_c of Mo-Ta superlattices as a function of the modulation wavelength λ . The triangles are the T_c values of samples fabricated under inferior sputtering conditions.

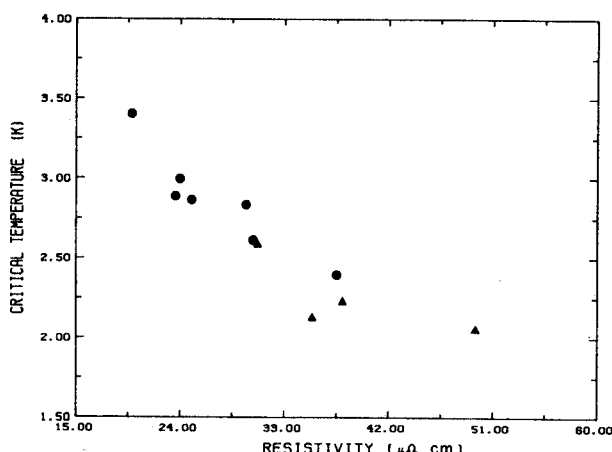


FIG. 3. Critical temperature T_c vs the electrical resistivity ρ at 4.2 K. The meaning of the symbols is the same as in Fig. 2.

value of ~ 3.2 K predicted by the dGW theory using bulk T_c and resistivity data. This deviation can be related to a shortened electronic mean free path causing a smeared density of states which determines a lowering in the density of states value at the Fermi energy.¹⁸

The electrical resistivity ρ of our samples was measured using a standard four-probe technique. The values were always in the metallic regime and the residual resistivity ratio, defined as $\beta=R(300 \text{ K})/R(4.2 \text{ K})$ was $\sim 1.2-1.4$ for all the wavelength values investigated. The behavior of ρ as a function of the wavelength λ confirmed a strong coupling between layers, with a high probability of the coherent passage of an electron across the interface.¹⁹

The samples fabricated under inferior sputtering conditions had higher values of the resistivity and lower values of T_c compared to the better samples with the same wavelengths. In Fig. 3 the critical temperature versus the resistivity at 4.2 K is plotted for all the Mo-Ta superlattices produced. The experimental points lay all on the same curve, showing the universal behavior of T_c versus ρ already found in $A15$ compounds, transition metals, and alloys.²⁰⁻²¹ This result indicates that, even for superlattices with a short-modulation wavelength, the resistivity is the single property relevant for determining T_c .

High-quality tunnel junctions were realized using two different procedures. In the first the Mo-Ta films were chemically etched to define a reliable base electrode geometry and then were sputter cleaned in an rf diode sputtering system with an argon pressure of 3.5 mTorr. All of the superlattices had a topmost layer of $\sim 200 \text{ \AA}$ of Ta. After the sputter cleaning process approximately 150 \AA of the top Ta layer was removed and the remainder was oxidized by heating the samples at 200°C for 30 sec. In the second procedure the samples were masked during the deposition and the geometrical definition of the tunnel junctions was obtained by a collodion technique after a thermal oxidation of several days at room temperature. In both procedures the second electrode was a thermal evaporated Pb film approximately 5000 \AA thick.

In Fig. 4, is shown the I - V characteristics of a tunnel junction at 1.5 K for a superlattice with $\lambda=58 \text{ \AA}$ as base electrode. Both procedures resulted in tunnel junctions

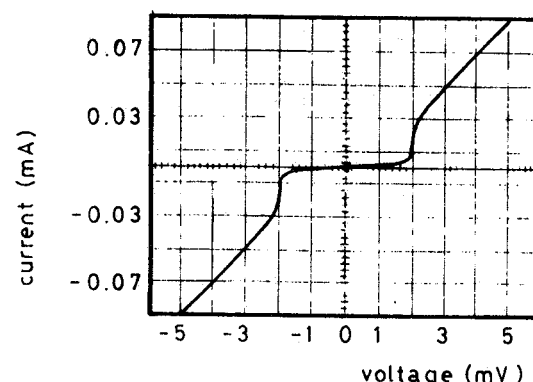


FIG. 4. I - V characteristic at $T=1.5$ K of a (Mo-Ta) $/Ta_xO_y/Pb$ tunnel junction. The superlattice used as a base electrode has $\lambda=58 \text{ \AA}$.

with very low leakage currents. The typical knee structure generally related to the proximity effect was always absent.

Standard tunneling techniques²² were used to measure the dV/dI versus V curve of our junctions in order to obtain the energy-gap values. Assuming the energy gap of Pb at $T=0$, $\Delta_{\text{Pb}}(0)=1.32$ meV, we calculated the value of the coupling strength constant, $2\Delta(0)/k_B T_c$, for our Mo-Ta superlattices to be ~ 3.5 . When the double-peak structure was present the two values of the coupling strength constant $2\Delta_1(0)/k_B T_c$ and $2\Delta_2(0)/k_B T_c$ were generally, respectively, around 3 and 4. At higher voltages, no superlattice phonon structures were detected confirming the weak coupling nature of the Mo-Ta superconducting superlattices.

In the modulation wavelength range 50–250 Å the dV/dI versus V curves showed a double-peak structure, as illustrated in Fig. 5 for a sample with $\lambda=82.2$ Å. The appearance of the double peak was independent of the normal resistance values of our junctions. We fitted the temperature behavior of these peaks using both proximity-effect theory²³ and two-band theory.²⁴ In Fig. 6, the temperature behavior of the two peaks for a superlattice with $\lambda=175$ Å is shown. The solid lines represent the best theoretical fit obtained using a proximity-effect theory.

We calculated the quasiparticle density of states

$$N_s(E) = \text{Re} \frac{|E|}{[E^2 - \Delta^2(E)]^{1/2}} \quad (1)$$

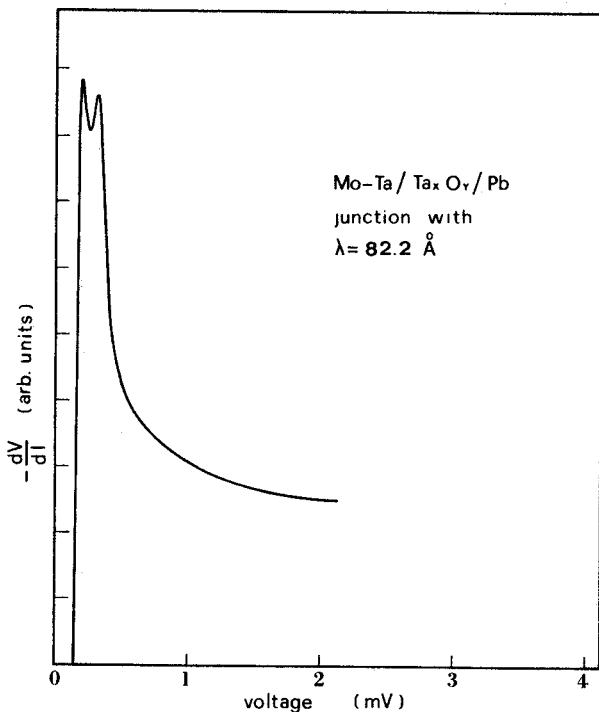


FIG. 5. $-dV/dI$ vs voltage V characteristic at $T=1.5$ K of a superlattice with $\lambda=82$ Å, showing the double-peak structure. The energy gap of Pb has been subtracted from the x scale.

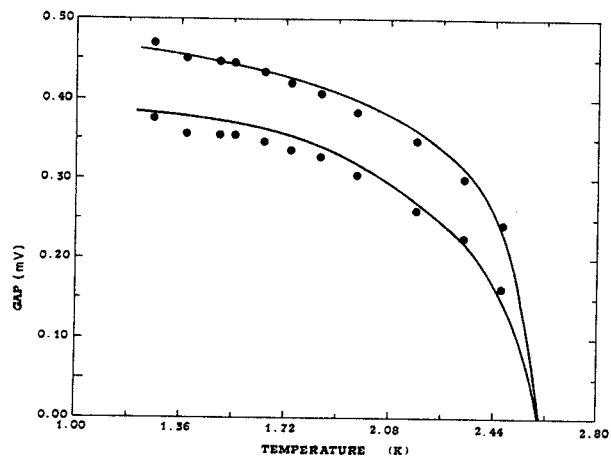


FIG. 6. Double-peak voltages as a function of the temperature of a superlattice with $\lambda=175$ Å. The solid lines are the best theoretical fit obtained with the proximity-effect theory (Refs. 23 and 25) using $\Gamma_N=0.035$, $\Gamma_S=0.14$, $\lambda_{\text{Mo}}=0.1971$, $\lambda_{\text{Ta}}=0.22$, and the bulk Debye temperatures.

from the self-consistency conditions for the BCS potentials at temperature $T\neq 0$,²⁵ obtaining the temperature behavior of the double peaks in $N_s(E)$. Values of the molybdenum λ_{Mo} and tantalum λ_{Ta} electron-phonon coupling constants were found to be very close to those calculated using bulk data from the BCS equation for T_c .²⁵ The best fit of our experimental curves was achieved with $\Gamma_N=0.035$ and $\Gamma_S=0.14$.

Figure 7 shows a curve of the quasiparticle density of states $N_s(E)$ as a function of the energy E , calculated using $\Gamma_N=0.001$ and $\Gamma_S=0.21$. The agreement with the data shown in Fig. 5 is good.

In Fig. 8, the experimental data of the two peaks as a function of the temperature are shown for a superlattice with $\lambda=50$ Å. In this case the solid lines are the best theoretical fit obtained by a two-band theory.

Indicating with A and B the gaps associated with the two bands, from the self-consistency conditions²⁴ we can write

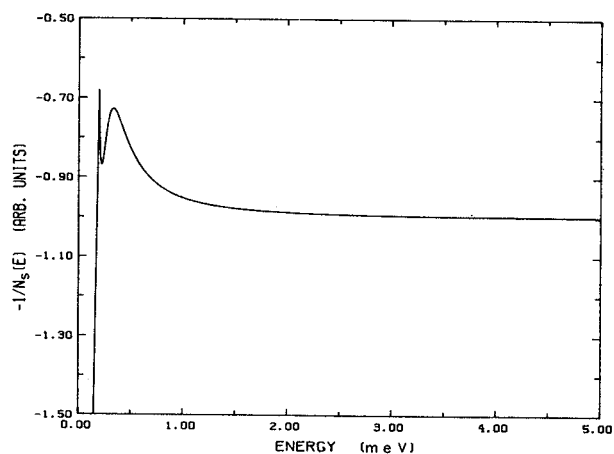


FIG. 7. The inverse of the quasiparticle density of states vs E by the proximity-effect theory (Refs. 23 and 25) using $\Gamma_N=0.001$ and $\Gamma_S=0.21$.

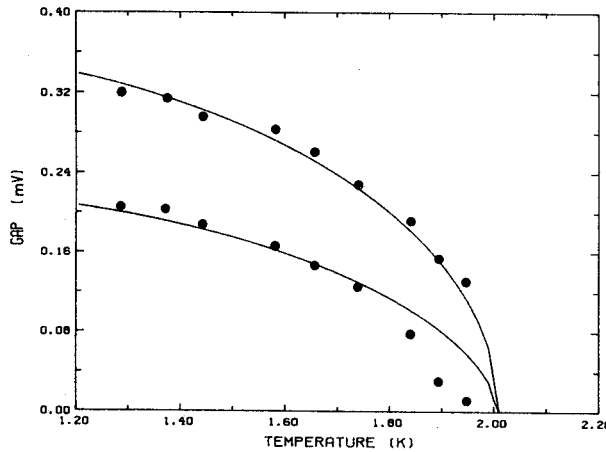


FIG. 8. Double-peak voltages as a function of the temperature of a superlattice with $\lambda = 50 \text{ \AA}$. The solid lines are the best theoretical fit using a two-band model (Ref. 24) with $V_A = 0.83$, $V_B = 10$, and an averaged Debye temperature of 359 K.

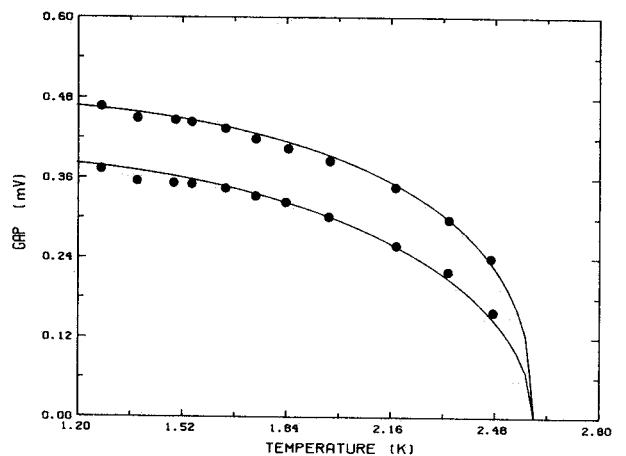


FIG. 9. Double-peak voltages vs temperatures of the same superlattice in Fig. 6. The solid lines represent the best fit using a two-band theory (Ref. 24) with $V_A = 1.22$, $V_B = 0.34$, and an averaged Debye temperature of 359 K.

$$B = AV_A\lambda_A F(A) + (A/V_B)[1 - \lambda_A F(A)], \quad (2)$$

where $\lambda_A = \lambda_S = N_{SS}(0)V_{SS}$ is the electron-phonon coupling constant for the s band electrons, $V_A = V_{Sd}/V_{SS}$ and $V_B = V_{Sd}/V_{dd}$, where V_{SS} , V_{dd} , and V_{Sd} are the averaged interaction energies, respectively, for s band, d band, and $s-d$ processes, and $F(A)$ is defined as

$$F(A) = \int_0^{k_B \vartheta_D} \left[\tanh \frac{(\epsilon^2 + A^2)^{1/2}}{2k_B T} \right] \frac{1}{(\epsilon^2 + A^2)^{1/2}} d\epsilon, \quad (3)$$

where ϑ_D is the Debye temperature.

From the BCS equation for T_c , we calculated λ_A using the measured critical temperature and an averaged bulk Debye temperature of 359 K.^{9,23} We obtained the best fit for our experimental data with $V_A = 0.83$ and $V_B = 10$.

In Fig. 9 is shown the best theoretical fit for the superlattice with $\lambda = 175 \text{ \AA}$, obtained from the two-band theory with $V_A = 1.22$ and $V_B = 0.34$.

The possibility of fitting our experimental data by using a two-band theory and a proximity-effect theory could be related to a similarity between the Hamiltonians

used in these theories. More detailed studies on this subject are in progress.

In conclusion, we fabricated bcc-bcc Mo-Ta superlattices in the modulation wavelength range 16–450 \AA with an equal number of atomic planes inside the single layers. The x-ray analysis indicated long structural coherence even in the limit of short-modulation wavelength, and the resistivity values were always in the metallic regime.

We realized high-quality tunnel junctions with two different procedures and the $2\Delta(0)/k_B T_c$ value was measured to be around 3.5 in all the Mo-Ta films. The T_c versus ρ curve showed a universal behavior and the dV/dI versus V curves for samples in the λ range 50–250 \AA showed a double-peak structure. The temperature behavior of these peaks was equally well fitted by using a two-band theory and a proximity-effect theory.

The work at the University of Arizona was supported by the Director, Office of Energy Research, Division of Materials Sciences, Office of Basic Energy Sciences, U.S. Department of Energy under Contract No. DE-FG02-87ER45297.

*Present address: Laboratori Nazionali di Frascati (LNF), Istituto Nazionale di Fisica Nucleare (INFN), Cassella Postale 13, I-00044 Frascati (Roma), Italy.

¹D. B. McWhan, *Synthetic Modulated Structures*, edited by L. L. Chang and B. C. Giessen (Academic, New York, 1985), Chap. 2.

²I. Banerjee, Q. S. Yang, C. M. Falco, and I. K. Schuller, Phys. Rev. B **28**, 5037 (1983).

³H. Homma, C. S. L. Chun, G. G. Zheng, and I. K. Schuller, Physica B + C **135B**, 173 (1985).

⁴K. Kanoda, H. Mazaki, T. Yamada, N. Hosoi, and T. Shinjo, Phys. Rev. B **33**, 2052 (1986).

⁵P. R. Broussard and T. H. Geballe, Phys. Rev. B **35**, 1664

(1987).

⁶J. P. Locquet, W. Sevenhuijsen, Y. Bruynseraede, H. Homma, and I. K. Schuller, IEEE Trans. Magn. MAG-23, 1393 (1987).

⁷R. Vaglio, A. M. Cucolo, and C. M. Falco, Phys. Lett. A **118**, 89 (1986).

⁸Q. S. Yang, C. M. Falco, and I. K. Schuller, Phys. Rev. B **27**, 3867 (1983).

⁹W. P. Lowe and T. H. Geballe, Phys. Rev. B **29**, 4961 (1984).

¹⁰J. Guimpel, M. E. de la Cruz, F. de la Cruz, O. Laborde, and J. C. Villegier, J. Low Temp. Phys. **63**, 151 (1986).

¹¹J. M. Triscone, D. Ariosa, M. G. Karkut, and O. Fischer, Phys. Rev. B **35**, 3238 (1987).

¹²R. Vaglio, A. M. Cucolo, and C. M. Falco, Phys. Rev. B **35**,

- 1721 (1987).
- ¹³J. L. Makous, C. M. Falco, R. Vaglio, and A. M. Cuocolo, Jpn. J. Appl. Phys. **26**, 1467 (1987).
- ¹⁴C. M. Falco, J. Phys. (Paris) Colloq. **45**, C5-499 (1984).
- ¹⁵H. P. Klug and L. E. Alexander, *X-Ray Diffraction Procedures*, 2nd ed. (Wiley, New York, 1974), Chap. 9.
- ¹⁶P. G. de Gennes and E. Guyon, Phys. Lett. **3**, 168 (1963).
- ¹⁷N. R. Werthamer, Phys. Rev. **132**, 2440 (1963).
- ¹⁸I. Banerjee, Q. S. Yang, C. M. Falco, and I. K. Schuller, Solid State Commun. **41**, 805 (1982).
- ¹⁹R. Dimmich, J. Phys. F **15**, 2477 (1985).
- ²⁰C. Camerlingo, P. Scardi, C. Tosello, and R. Vaglio, Phys. Rev. B **31**, 3121 (1985).
- ²¹P. W. Anderson, K. A. Muttalib, and T. V. Ramakrishnan, Phys. Rev. B **28**, 117 (1983).
- ²²J. M. Rowell, *Tunneling Phenomena in Solids*, edited by E. Burstein (Plenum, New York, 1969).
- ²³W. L. McMillan, Phys. Rev. **175**, 537 (1968).
- ²⁴H. Suhl, B. T. Matthias, and L. R. Walker, Phys. Rev. Lett. **3**, 552 (1959).
- ²⁵J. Vrba and S. B. Woods, Phys. Rev. B **3**, 2243 (1971).